EUV two-photon-ionization cross sections of helium from the solution of the time-dependent Schrödinger equation, and comparison with measurements using free-electron lasers

Theodoros Mercouris,* Yannis Komninos,† and Cleanthes A. Nicolaides‡
Theoretical and Physical Chemistry Institute, National Hellenic Research Foundation, 48 Vasileos Constantinou Avenue, Athens 11635, Greece

(Received 16 June 2016; published 8 December 2016)

Two recent experimental papers reported the first measurements of *absolute* two-photon-ionization cross sections $\sigma(2)$ of helium, for EUV wavelengths, using free-electron laser (FEL) pulses [Sato *et al.*, J. Phys. B **44**, 161001 (2011); Fushitani *et al.*, Phys. Rev. A **88**, 063422 (2013)]. The wavelengths correspond to transitions that are off resonance as well as on resonance with the $1s2p$ and $1s3p\ ^1P^o$ Rydberg states. Inspection of their results reveals considerable discrepancies, while their comparison with theoretical results obtained earlier from time-independent calculations, one perturbative and two nonperturbative ones, cannot lead to secure conclusions as to the true values of $\sigma(2)$. We examined this prototypical problem by implementing a time-dependent approach, which utilizes the nonperturbative solution of the time-dependent Schrödinger equation. This solution was obtained in terms of the state-specific expansion approach, in an upgraded version where the coupling matrix elements are computed using the *full electric* operator of the multipolar Hamiltonian. The $\sigma(2)$ were obtained for pulses of 300 fs, as in the 2011 FEL experiment. Their computation was achieved by fitting the time-dependent ionization survival probability to $e^{-\Gamma t}$, where Γ is the rate of ionization. The wavelengths and intensities are those of the FEL experiments, as well as others, such as the wavelengths 52.22 and 51.56 nm, for which the $1s4p\ ^1P^o$ and $1s5p\ ^1P^o$ levels are on resonance with the initial ^1S state. Apart from the predictions for these wavelengths, the paper contains characteristic comparisons among all the results on these EUV $\sigma(2)$, experimental and theoretical. In general, the trends predicted by nonperturbative methods are confirmed by the FEL measurements. However, discrepancies exist among the absolute numbers. Furthermore, comparison among the results of the three nonperturbative approaches (present time-dependent and two earlier time-independent ones published in 1999 and 2005) indicates an overall consistency, although quantitative differences for individual cases are apparent.

DOI: 10.1103/PhysRevA.94.063406

I. TWO RECENT EXPERIMENTS USING EUV FREE-ELECTRON LASER

The quantitative description of the interaction of strong pulses with atomic and molecular states is a very demanding and challenging many-electron problem. Its solution presupposes the existence of suitable theories and appropriate formalisms that not only explain the phenomenology in a descriptive way, but also, and especially, allow the credible and accurate calculation of the observable quantities. In all cases, the success of this general goal hinges on the possibility of incorporating and handling computationally the key electronic structures and the corresponding electron correlations of the states contributing the most to the phenomenon under consideration, and of providing a transparent picture of the interplay between the parameters of the pulses and the characteristics of the spectra. In this endeavor, the exchange of *quantitative* information between theory and experiment is indispensable.

For example, in the quantitative study of multiphoton-ionization (MPI) phenomena, as the field strength (intensity) increases the *a priori* adoption of the conventional lowest-order perturbation theory (LOPT) approach loses its formal credibility, since, at some unknown point, higher-order terms may start contributing in a significant way. This is the boundary between *weak* and *strong* fields, where the LOPT formula starts breaking down even if the calculation is (could be) done accurately. For each problem of interest (many-electron states plus laser parameters), the prediction and quantitative understanding of this breakdown is quantitatively vague and precarious without systematic many-electron theory and computations which are *nonperturbative* and which can be implemented with sufficient accuracy. By "nonperturbative" it is meant that the formalism and the calculations of a particular property incorporate, at least in principle, the significant contributions from the interactions described by the *total* Hamiltonian to all orders of perturbation theory. In fact, only then, by comparing results as the field strength is increased, can one assess the relevance and/or the degree of reliability of properly executed LOPT calculations for the same parameters of the pulse. Obviously, accurate experimental information, which in principle may become available, is the alternative or complementary reference point for the assessment of the limits of applicability and relevance of LOPT for each problem.

The helium atom has a ground state with a very simple electronic structure, labeled by the single-determinantal configuration $1s^2\ ^1S$, while its energy spectrum has channels of Rydberg or scattering states as well as doubly excited states (DES) above its ionization threshold of 24.59 eV. As such, it offers convenient opportunities for theoretical and experimental studies of important aspects of MPI caused by the interaction with electromagnetic pulses with various values of field strength, of duration, and of wavelength.

*thmerc@eie.gr
†ykomn@eie.gr
‡caan@eie.gr

Two recent publications [1,2] reported results of the first measurements of the *absolute* cross sections for the two-photon ionization of helium by free-electron laser (FEL) extreme-UV (EUV) pulses. The values of the intensity were 3×10^{12} W/cm^2 in [1] and in the range 5×10^{12}–5×10^{13}, with emphasis on 1×10^{13} W/cm^2, in [2]. The wavelengths were in the range 53–62 nm. The pulse duration was estimated to be about 100 femtoseconds (fs) in [1] and about 300 fs in [2].

Although both groups utilized the same FEL facilities in Japan, the experimental techniques for measurement are different. According to Fushitani *et al.* [1], their technique, namely the "shot-by-shot" analysis of photoelectron spectra, produced results that are more reliable than those reported in 2011 by Sato *et al.* [2], since it corrects for the "jitter" that afflicted the earlier measurements. For example, when discussing the case of the nonresonant ionization measured in their two-color experiment, they state, "... we obtain a jitter-free cross section for nonresonant two-color two-photon ionization of He, $\sigma(2)\,\mathrm{He}(20.8\,\mathrm{eV}, 4.63\,\mathrm{eV}) = 4.1(6) \times 10^{-52}$ cm^4 s, from Eq. (7). It should be noted that without the timing-jitter correction, we obtain a significantly smaller value, $1.6(3) \times 10^{-52}$ cm^4 s"(p. 5 of [1]).

Discrepancy between results of the two experiments [1,2] is observed for other cases as well. It underlines the fact that such FEL measurements are new and under evolving understanding of their quantitative details (e.g., concerning the precise characteristics of the pulses as they interact with the atomic or molecular state of interest).

Apart from the issue of the level of accuracy of the FEL measurements of MPI absolute cross sections for wavelengths in the EUV and beyond, there is also another significant aspect in [1,2] which contributed to our motivation to carry out the present work. This has to do with the fact that measurements such as those of [1,2] allow the assessment of formalisms and of related methods for the calculation from first principles of quantities representing the physics of the nonlinear response of atoms and molecules to *high-frequency* strong pulses.

Indeed, in both papers [1,2], and especially in [2], the authors compared their results for the one-color, two-photon absolute cross section $\sigma(2)$ with theoretical ones that were published in 2001 [3] and in 2005 [4]. The results of Nikolopoulos and Lambropoulos [3] were obtained from calculations that used the formula of LOPT. The calculations of van der Hart and Bingham [4] go beyond LOPT. They applied the time-independent nonperturbative "*R*-matrix Floquet" theory, introduced and demonstrated in the 1990s; see references in [4]. Comparison of the two sets of results is made in Table II of [2] and is repeated in our Table I.

To the results and corresponding conclusions in [1–4] on the helium EUV $\sigma(2)$, here we add those published in 1999 by Mercouris *et al.* [5], which are missing from the reference lists of [1–4]. In fact, the main conclusions stated by Sato *et al.* [2] regarding the behavior of $\sigma(2)$ as a function of increasing intensity are consistent with the predictions made in [5]. However, there are discrepancies of quantitative nature; see the next section. The results of [5] were obtained via the non-Hermitian, time-independent, nonperturbative "many-electron, many-photon" theory (MEMPT), which was first introduced and applied in the late 1980s; see references in [5].

TABLE I. Two-photon-ionization cross sections of He, $\sigma(2)$, for four EUV wavelengths and for peak intensity 1×10^{13} W/cm^2, in units of 10^{-52} cm^4 s. The values 58.4 and 53.4 nm are on resonance with the $1s2p$ and $1s3p\,{}^1P^o$ Rydberg states. Two recent FEL measurements [1,2] are compared with the theoretical results of [3] (LOPT) and of [4] (*R*-matrix Floquet). The significant discrepancies motivated the present theoretical work, which is based on the nonperturbative solution of the METDSE using the SSEA. (The SSEA results are listed in Table III). Additional results from nonperturbative time-independent MEMPT calculations [5] are presented in Table II; see text.

λ (nm)	61.4	58.4	56.0	53.4
Experiment [2]	2.6(6)	23(7)	0.9	7(5)
Experiment [1] (extrapolated from 3×10^{12} W/cm^2)		150(30)		
Theory (time-independent)				
LOPT [3]	8.0	360	2.7	
R-matrix Floquet [4]	8.5	63	3.5	6.9

The main results of [1–5] and their comparison regarding the EUV $\sigma(2)$ are put together in Sec. II.

The three theoretical investigations [3–5], implemented formalisms that are *time independent*, implying that the pulse is sufficiently long so as to produce an averaged result. The present approach is nonperturbative and *time dependent*, using pulses whose duration follows from those used in the experiments. It is based on the direct solution, $\Psi(q,t)$, of the many-electron time-dependent Schrödinger equation (METDSE), which is obtained by implementing the state-specific expansion approach (SSEA) [6,7].

The $\sigma(2)$ have been extracted by fitting the time-dependent probability, $P(t)$, of the atom remaining in states of the discrete spectrum, to the form $e^{-\Gamma t}$, where Γ is the rate of ionization. The pulses are of $\sin^2$ shape and have duration of 300fs, with ramp-on and ramp-off parts of 20 cycles. The peak intensity is in the range 3×10^{12}–1×10^{14} W/cm^2, for the EUV wavelengths that were used in the FEL experiments [1,2]. These wavelengths correspond to nonresonant ionization as well as to ionization that evolves resonantly, via the transition to the $1s2p$ ($\lambda = 58.4$ nm) or the $1s3p$ ($\lambda \approx 53.4$ nm) ${}^1P^o$ Rydberg states.

We also calculated $\sigma(2)$ for $\lambda = 52.22$ nm ("weak" field of 3×10^{12} W/cm^2) and for 51.56 nm ("strong" field of 1×10^{14} W/cm^2), which bring on resonance the $1s4p\,{}^1P^o$ and $1s5p\,{}^1P^o$ Rydberg states with the initial ground state. These predictions can be tested in future FEL experiments.

II. CRITICAL ASSESSMENT OF THE EXPERIMENTAL AND THEORETICAL RESULTS REPORTED IN [1–5]

In Sec. I, we drew attention to Fushitani *et al.* [1], whose arguments imply that, in the emerging experiments using high-energy FEL, there are still critical points regarding the conditions and techniques that are needed to guarantee the credibility of measured quantities concerning the MPI of atoms and molecules. At the same time, the comparison with earlier

theoretical results [3,4] which was made in [1,2] suggests that there is need for additional quantitative information. We glean the following examples from [1,2].

Fushitani *et al.* [1] measured $\sigma(2) = 5(\pm 1) \times 10^{-50}\,\mathrm{cm}^4\,\mathrm{s}$, with a pulse of about 100 fs, at $\hbar\omega = 21.2\,\mathrm{eV}$ and intensity $I = 3 \times 10^{12}\,\mathrm{W/cm}^2$. The energy $\hbar\omega = 21.2\,\mathrm{eV}$ (wavelength 58.4 nm) is on resonance with the $1s2p\ ^1P^o$ state. Based on reasonable arguments, they extrapolated to $I = 1 \times 10^{13}\,\mathrm{W/cm}^2$ and obtained $\sigma(2) = 15(\pm 3) \times 10^{-51}\,\mathrm{cm}^4$ s. They wrote that this value "agrees" within a factor of ~2.5 with the theoretical value of the *R*-matrix Floquet calculation [4], which is $\sigma(2) = 6.3 \times 10^{-51}\,\mathrm{cm}^4$ s. Also, they referred to the previous experiment of Sato *et al.* [2] and stated, "Recently, a smaller experimental value, $2.3(7) \times 10^{-51}\,\mathrm{cm}^4$, was reported by ion-mass spectrometry using FEL [2]. The origin of the large discrepancy from the present value is not clear, but it is partly attributed to the temporal integration factors $T(1)$ and $T(2)$ omitted in the previous study."

In addition, the comparison first published by Sato *et al.* [2], and repeated in our Table I, between their measurements and the theoretical results of [3,4], also reveals quantitative differences. For example, for $I = 1 \times 10^{13}\,\mathrm{W/cm}^2$ and wavelength $\lambda = 56\,\mathrm{nm}$, which is not on resonance with a discrete state, Sato *et al.* [2] determined $\sigma(2) = 0.9 \times 10^{-52}\,\mathrm{cm}^4$ s, whereas the theoretical results are $2.7 \times 10^{-52}\,\mathrm{cm}^4$ s [3] and $3.5 \times 10^{-52}\,\mathrm{cm}^4$ s [4]. On the other hand, again for $I = 1 \times 10^{13}\,\mathrm{W/cm}^2$ but for the on-resonance wavelength $\lambda = 58.4\,\mathrm{nm}$, the value produced by the LOPT calculation of [3] is $360 \times 10^{-52}\,\mathrm{cm}^4$ s, in striking disagreement with that of [4], which gave $63 \times 10^{-52}\,\mathrm{cm}^4$ s.

For the reader's convenience, the results on the He $\sigma(2)$ that were compared in [1,2], are collected in our Table I. We note that for the wavelength of 53.4 nm ($\hbar\omega = 23.2\,\mathrm{eV}$), the uncertainty in the measurements is large, and so their comparison with the theoretical results [3,4] cannot be conclusive.

A. Higher-order effects. Additional information from the early study of the problem via the MEMPT [5]

In order to complete the critical assessment of the available information on the EUV $\sigma(2)$ of helium, we recall a subset of the predictions made in [5] using the MEMPT, which is a time-independent approach formulated as a non-Hermitian problem for field-induced resonance states decaying into the continuum (see the review [8]).

The nonperturbative calculations in [5] permitted, among other things, the identification of regions of values of frequencies and intensities where the validity of LOPT for the I^k power "law" breaks down when the multiphoton process does not encounter intermediate states (Table I of [5]). In addition, the effects of intermediate states (a theme that is discussed in the experimental papers [1,2]), or of states that cannot participate in LOPT, were also explored quantitatively.

The above statement, apart from its general scope, covers material that was also discussed in [4] and in [1,2], and so we elaborate on it by giving an example:

Figure 5 of [5] depicts the two-photon-ionization rate of He as a function of frequency and of intensity. A characteristic feature is that, for about $\hbar\omega = 20.1\,\mathrm{eV}$ and as the intensity increases beyond about $3.5 \times 10^{12}\,\mathrm{W/cm}^2$, a peak emerges from the smooth background, while the structure due to $1s2p\ ^1P^o$ starts decreasing and, at larger intensities, eventually disappears. The peak in the continuous spectrum is "a manifestation of a higher-order effect, whereby the autoionizing state $2s2p\ ^1P^o$, whose field-free position is 60.2 eV, is coupled resonantly with the He ^1S ground state via a three-photon process" (p. 9 of [5]). In other words, even though in lowest order the two-photon-ionization process from the ^1S state reaches only ^1S and ^1D states of even parity, as field intensity increases the higher-order aspect of dynamics manifests itself via, on the one hand, the disappearance (due to coupling with the ^1S states) of the structure corresponding to the $1s2p\ ^1P^o$ intermediate state and, on the other hand, the appearance of the lowest $^1P^o$ DES inside the continuous spectrum.

Such results and conclusions were also reported in [4] (e.g., compare Fig. 5 of [5] with Fig. 4 of [4]), based again on nonperturbative calculations. Indeed, van der Haart and Bingham confirmed our earlier observations, which were recalled in the previous paragraph, by stating, "... the figure clearly demonstrates that excitation of the resonance ($2s2p\ ^1P^o$) is a higher-order process: with increasing intensity the resonance becomes more pronounced." (p. 241 of [4]).

The theoretical prediction [5] that, when the wavelength is on resonance with the $1s2p\ ^1P^o$ state the cross section decreases as the intensity increases, was observed experimentally [2].

Furthermore, according to the results of [4,5], when the intensity increases beyond $10^{13}\,\mathrm{W/cm}^2$, the accurate determination of $\sigma(2)$ becomes more complicated and demanding, especially if the photon energy reaches $1snp\ ^1P^o$ states with $n \geqslant 3$, and the results become very sensitive to the mixing of states and to the details of their wave functions. This complexity must be reflected in measurements as well.

For reasons of economy, we do not discuss additional cases. Instead, we converted to $\sigma(2)$ the values given in the graphs of [5] as rates, and prepared Table II, which includes the experimental $\sigma(2)$ [1,2]. The MEMPT calculations were done for seven values of intensity: 3.5×10^{12}, 1.4×10^{13}, 3.15×10^{13}, 5.6×10^{13}, 8.75×10^{13}, 1.26×10^{14}, and $1.72 \times 10^{14}\,\mathrm{W/cm}^2$. Fortunately, they included two of the wavelengths that were used in [1,2], and so comparison can be made. These are 61.4 nm (off resonance with an intermediate $^1P^o$ state) and 58.4 nm (on-resonance with the $1s2p\ ^1P^o$ state).

Although the reader can draw conclusions by inspecting Table II, we note, as an example, that for 58.4 nm and $I = 3.5 \times 10^{12}\,\mathrm{W/cm}^2$, the MEMPT value is $156 \times 10^{-52}\,\mathrm{cm}^4$ s, about a factor of 3 smaller than the experimental one at the slightly lower $I = 3 \times 10^{12}\,\mathrm{W/cm}^2$, which is $500(\pm 100) \times 10^{-52}\,\mathrm{cm}^4$ s [1]. At $1.4 \times 10^{13}\,\mathrm{W/cm}^2$, the result from the *R*-matrix Floquet calculations [4], $\sigma(2) = 63 \times 10^{-52}\,\mathrm{cm}^4$ s, is consistent with the MEMPT value, $\sigma(2) = 44.5 \times 10^{-52}\,\mathrm{cm}^4$ s.

In conclusion, the rough quantitative picture of the helium $\sigma(2)$ emerging from the FEL experiments [1,2] and from the time-independent calculations of [3–5] is the following:

Regarding wavelength-dependent trends and intensity-dependent higher-order effects, the predictions from our earlier nonperturbative study [5] have been confirmed during the past 15 years by both the calculations of [4] and the recent measurements [1,2].

TABLE II. Collection of results from [1,2,5] on the helium $\sigma(2)$, in units of 10^{-52} cm^4 s, for wavelengths 61.4 nm (off resonance) and 58.4 nm (on resonance with the $1s2p\,^1P^o$ Rydberg state). The values from the FEL experiments [1,2] are for peak intensities 3×10^{12} W/cm^2 and 1×10^{13} W/cm^2. The nonperturbative MEMPT values from figure 5 of Ref. [5], published here as numbers, were obtained for seven values of intensity, in the range 3.5×10^{12}–1.715×10^{14}. For the off-resonance wavelength, $\lambda = 61.4$ nm, the MEMPT results exhibit the constancy expected from LOPT.

λ (nm)	61.4	58.4
Experiment [1]		
3×10^{12} W/cm^2		500(100)
1×10^{13} W/cm^2		150(30)
(extrapolated from 3×10^{12} W/cm^2)		
Experiment [2]		
1×10^{13} W/cm^2	2.6(6)	23 (7)
Theory (MEMPT) [5]		
3.5×10^{12} W/cm^2	9.3	156
1.4×10^{13} W/cm^2	9.3	44
3.15×10^{13} W/cm^2	9.0	23
5.6×10^{13} W/cm^2	8.7	15
8.75×10^{13} W/cm^2	8.5	11
1.26×10^{14} W/cm^2	8.3	9
1.72×10^{14} W/cm^2	8.7	8

However, when it comes to quantitative answers, for cases where the wavelength is on resonance with a Rydberg state and/or the field intensity starts getting strong, there are challenging open issues. This is because the FEL measurements [1,2] disagree with each other, while, in characteristic cases, both deviate significantly from the time-independent calculations of [3–5] (Tables I and II).

The present work is aimed at obtaining quantitative information for the $\sigma(2)$ of helium by EUV photons, in terms of a nonperturbative approach which is *time dependent*. The theory uses a pulse of finite duration, just like the FEL measurement does. This task is important in its own right. At the same time, given the aforementioned existing uncertainty as to what values of $\sigma(2)$ represent reality more closely, it is expected that the results will be helpful to current research with FEL measurements of MPI cross sections of many-electron atoms and ions.

III. CALCULATION OF THE HELIUM EUV $\sigma(2)$

The problem at hand is to extract the $\sigma(2)$ from a description which includes the time-dependent interaction of the initial state of helium with weak or strong pulses of EUV wavelengths with duration of about 300fs. Some of the frequencies are on resonance with the excitation energies to Rydberg states $1snp\,^1P^o$, $n = 2,3,4,5$, while their intensities are high enough so as to induce nonlinear effects from real and virtual transitions in the discrete and the continuous spectrum, the latter labeled by $1s\varepsilon\ell$, $\ell = 0,1,2,\ldots$.

The approach that we adopted, which is validated by the results which are presented in the next section, was to compute nonperturbatively the corresponding time-dependent probabilities for the system to remain in the discrete spectrum, $P(t)$, and to average by fitting them to $e^{-\Gamma t}$, where Γ is the ionization rate. From the rate one obtains $\sigma(2)$.

Accordingly, first and foremost the theory requires the accurate solution $\Psi(t)$ of $\boldsymbol{H}(t)\Psi(t) = i\hbar\frac{\partial\Psi(t)}{\partial t}$, for a time-dependent Hamiltonian,

$$\boldsymbol{H}(t) = \mathbf{H}_{\rm He} + \boldsymbol{V}(\omega,t), \tag{1}$$

where $\boldsymbol{V}(\omega,t)$ is the interaction operator containing the relevant characteristics of the pulse. The following paragraphs describe the main features of our approach towards this goal.

A. State-specific expansion approach (SSEA)

The solution $\Psi(\vec{r}_1, \vec{r}_2, t)$ was calculated via the SSEA, which was introduced in the early 1990s as a systematic and general methodology for the nonperturbative solution of the METDSE. It has been reviewed recently in [6,7]. We outline its main characteristics and connect them to the present calculation.

The theoretical foundation is the quantum mechanical principle of the expansion of a many-electron nonstationary state, $\Psi(t)$, in terms of the complete set of stationary states of the discrete and the continuous spectrum of the atomic (molecular) Hamiltonian, with time-dependent complex coefficients. When it comes to implementation to real, N-electron systems, the crucial requirement is that this expansion be represented by wave functions which are *state specific*. Hence, the initial state, and the multitude of excited discrete and, especially, scattering states, which are of significance to the problem, enter into the expansion in terms of wave functions which have been optimized to represent each one of them as well as possible.

The initial state may have an arbitrary electronic structure, since the formalism is not restricted to simple closed-shell, single-determinantal singlet states. For each bound state in the expansion, the wave function is constructed and computed according to the scheme "state-specific Hartree-Fock (HF) or multiconfigurational HF (MCHF) plus the remaining important electron-correlation components of the wave function." The level and the method of the calculation depend on the state. Descriptions and references regarding the *state- and property-specific theory* and its methodologies for the production of such wave functions can be found in [6–8].

Since the SSEA requires the use of state-specific N-electron wave functions, each obtained in terms of its own function space, it allows one to first make an approximate analysis of the apparent requirements in terms of the characteristics of the spectrum of the stationary states and of the pulse. Accordingly, the N-electron SSEA wave function $|\Psi_{\rm SSEA}(t)\rangle$ is constructed and computed in the form (we omit the index for each possible channel)

$$|\Psi_{\rm SSEA}(t)\rangle = \sum_m a_m(t)|m\rangle + \int_0 b_\varepsilon(t)|\varepsilon\rangle d\varepsilon. \tag{2}$$

The $|m\rangle$ represent the relevant state-specific bound N-electron wave functions and the $|\varepsilon\rangle$ are energy-normalized, state-specific, scattering (free) wave functions. Resonance states are represented by their localized (bound) component.

The choice of the wave functions in Eq. (2) for each stationary state of physical significance and their numerically reliable calculation constitute the backbone of our proposal for the nonperturbative solution of the METDSE from first principles.

Substitution of (2) into the METDSE produces a system of integrodifferential coupled equations containing energies, *bound-bound*, *bound-free*, and *free-free* matrix elements, and the unknown complex coefficients. For the present problem, the number of equations was 10 030.

In the process of the solution of this system of equations for each point in time [6], one can monitor and evaluate with transparency and economy the dependence of the evolution of $|\Psi_{\rm SSEA}(t)\rangle$, and of the final quantity of interest, on each $|m\rangle$ and $|\varepsilon\rangle$. For example, one may follow the effect of a particular Rydberg state by including its wave function in Eq. (2) or by taking it out. For reasons of accuracy, in the case of atoms the Rydberg wave functions are obtained *numerically*, as solutions of the state-specific HF equations, with a term-dependent (N–1)-electron core. Rydberg states affect the physics of valence-electron excitation mainly via their outer electron, and so they may be considered as being effectively one-electron systems for a given term-dependent potential. Nevertheless, additional care must be taken so as to achieve good numerical accuracy in the asymptotic region.

Of special importance is the proper representation of the multichannel (in general) continuous spectrum, especially when the field becomes strong and all types of transition couplings on and off resonance occur. As regards radial accuracy for each angular momentum, the channel-dependent, energy-normalized scattering orbitals are calculated in the potential of the term-dependent HF (N–1)-electron core. As regards the effect of angular momentum states in the continuum, convergence tests lead to the final choice of their number. An example of their significance in nonperturbative calculations was demonstrated some time ago in the case of MPI of helium by strong laser pulses of 5 eV [9].

For the present problem, the SSEA wave function was constructed in the form

$$\Psi_{\rm SSEA}(t) = \sum_{\ell=0,n=\ell+1} a_{n,\ell}(t)\Phi(1sn\ell\,^1L) + \sum_{\ell=0}\int d\varepsilon a_{\varepsilon,\ell}(t)\Phi(1s\varepsilon\ell\,^1L). \quad (3)$$

At $t=0$, the coefficient of the initial, ground-state wave function $\Phi(1s^2\,^1S)$ is $a_{1,0}(0)=1$. This wave function was obtained from a numerical MCHF calculation consisting of the $1s^2$, $2s^2$, $2p^2$, $3s^2$, $3p^2$, $3d^2$, $4s^2$, $4p^2$, $4d^2$, and $4f^2$ configurations. The first three coefficients are the most important: 0.996, -0.062, and 0.062.The other discrete states, $1sn\ell$, are represented by numerical HF wave functions, with $\ell = 0,\ldots,4$ and $n = 2,3,4,5,6,7$. As we have already mentioned above and in earlier publications, it is important for problems such as the one treated here to use numerically accurate Rydberg wave functions, since, for frequencies on resonance they act as real intermediate states and the corresponding matrix elements must be accurate.

The energies of the scattering orbitals $\varepsilon\ell$ were in the range from 0 to 2.0 a.u. above threshold with $\ell = 0,\ldots,4$. The energy step was 0.001 a.u. Given the pulse parameters and the problem of interest, it was unnecessary to include doubly excited states embedded in the continuum. Time propagation was done on steps from 0.1 to 0.01 a.u., depending on the magnitude of the intensity.

Once the coefficients $a_{n,\ell}(t)$ and $a_{\varepsilon,\ell}(t)$ have been calculated, the MPI survival probability (probability for the system remaining in the discrete spectrum) is given in a transparent and accurate way by

$$P(t) = \sum_{n,\ell} |a_{n,\ell}(t)|^2 = 1 - P_{\rm ion}(t), \quad (4)$$

where the summation is restricted to the bound (Rydberg) states of He and $P_{\rm ion}(t)$ symbolizes the ionization probability.

B. Choice and treatment of the interaction operator

An innovation that was introduced in the present SSEA calculation is the use in $\boldsymbol{V}(\omega,t)$ of the *full electric* operator, $H_{el}(\omega,t)$, of the *multipolar* Hamiltonian, $\boldsymbol{H}_{\rm MP}(t)$, in terms of which the bound-bound, bound-free, and free-free coupling matrix elements were calculated. An excellent source for the description of the formal characteristics of $\boldsymbol{H}_{\rm MP}(t)$ are the treatises [10,11].

Our initial point of reference is the expression for the *full* electric operator, written here as $H_{el}(\omega,t)$, which is given in Eq. (5.35) of [10]:

$$H_{el}(\omega,t) = e\sum_j \int_0^1 \vec{r}_j\cdot\vec{E}(t,\lambda\vec{\kappa}\cdot\vec{r}_j)d\lambda, \quad (5)$$

where $\vec{\kappa}$ is the wave vector of the EUV pulse ($\kappa=\omega/c$), and j sums over the electrons. $\vec{E}(t,\lambda\vec{\kappa}\cdot\vec{r}_j)$ is the electric field and λ is a dummy variable.

In a series of papers, e.g., [12,13] and references therein, we have shown how this Hamiltonian [Eq. (5)] can be reduced to forms which are suitable for computation of matrix elements with numerical bound as well as authentic (i.e., energy normalized with correct asymptotic boundary conditions) scattering wave functions in spherical symmetry, as used, e.g., in atomic physics.

The key reasons for the choice of $\boldsymbol{H}_{\rm MP}(t)$ as the perturbing interaction operator are, briefly, the following:

(1) The theoretical necessity to use, instead of the conventional electric dipole approximation (EDA), the *full* atom-radiation interaction for the solution of the METDSE, comes to the forefront not only for cases where the radiation wavelength becomes very small, but also for MPI processes where the interactions between extended wave functions, such as those of high-n Rydberg states and of the unbound orbitals of scattered states, may play a crucial role. In this case, the conventional argument leading to the adoption of the EDA, i.e., invoking the "dimensions" of the atom with respect to the radiation wavelength, cannot be justified *a priori*.

(2) In the SSEA, the energy-normalized scattering orbitals are computed and used numerically, subject to the rigorous asymptotic boundary conditions. When it comes to the numerical calculation of *free-free* matrix elements, on and off resonance, one is faced with the calculation of integrals over unbound, strongly oscillatory numerical functions, multiplied

by (N–1)-electron overlap integrals. Singularities occur as $\varepsilon \to \varepsilon'$, where ε and ε' are the free-electron energies in two different orbitals. Since for strong-field problems the number of free-free matrix elements (on and off resonance) may be huge, no discounts on their numerical accuracy ought to be made, if the final result is to be considered reliable. Therefore, it is important for theory to account for these singularities accurately and consistently. We have shown [12,13] that the mathematical structure of the free-free matrix elements of $H_{el}(\omega,t)$, on and off resonance, is simpler than that of its EDA limit, which is the r operator. Therefore, it is easier to handle numerically and accurately.

(3) Apart from the preceding reasons having to do with the mathematics and computation of free-free matrix elements of energy-normalized scattering functions, there is also a fundamental quantum mechanical reason for choosing $\boldsymbol{H}_{\rm MP}(t)$ when it comes to the nonperturbative solution of the METDSE from first principles. It has to do with the issue of the possible gauge dependence of the sought-after quantity [14–16]. We have explained in [12,13] and their references, that the choice of $\boldsymbol{H}_{\rm MP}(t)$, which contains the gauge-invariant electric field, and the use of $H_{el}(\omega,t)$ in the METDSE, guarantees that the time-dependent complex coefficients in the expansion (2) can be interpreted directly as probability amplitudes.

IV. RESULTS

The calculations were done for a laser-pulse envelope,

$$g(t) = \begin{Bmatrix} \sin(\pi t/2T_r)^2 & 0 \leqslant t \leqslant T_r \\ 1 & T_r \leqslant t \leqslant T_f \\ \sin[\pi(t - T_f + T_{\rm off})/2T_{\rm off}]^2 & T_f \leqslant t \leqslant T_f + T_{\rm off} \end{Bmatrix}, \tag{6}$$

where T_r is the time during which intensity rises, $(T_f - T_r)$ is the period with constant intensity, and $T_{\rm off}$ is the interval in which intensity falls to zero.

We obtained the two-photon-ionization rate $\Gamma(\omega,F)$ by performing a nonlinear fitting of $e^{-\Gamma t}$ to the time-dependent curve of the survival probability.

The relationship between $\Gamma(\omega,F)$ and the cross section is

$$\sigma(n) = \omega^n[\Gamma(\omega,F)/\hbar]/I^n, \tag{7a}$$

in units of $\mathrm{cm}^{2n}\,\mathrm{s}^{n-1}$. Therefore, for two-photon ionization, the cross section $\sigma(2)$ is given by

$$\sigma(2) = \left(\frac{\omega}{I}\right)^2 \Gamma(\omega,F)7.857 \times 10^{-19}\,\mathrm{cm}^4\,\mathrm{s}, \tag{7b}$$

in which ω and Γ should be given in a.u. and I in $\mathrm{W\,cm}^{-2}$.

Figure 1 depicts the survival probability $P(t)$ of Eq. (4), for $\lambda = 58.4\,\mathrm{nm}$ and $I = 10^{13}\,\mathrm{W\,cm}^{-2}$. The thick gray line corresponds to the fitted exponential form, $e^{-\Gamma t}$, with $\Gamma = 1.05 \times 10^{-6}$ a.u. According to Eq. (7b) this value gives $\sigma(2) = 50.2 \times 10^{-52}\,\mathrm{cm}^4\,\mathrm{s}$.

The oscillations of $P(t)$ are a manifestation of the Rabi oscillation between the He ground state, $1s^2$, and the excited state $1s2p\,{}^1P^o$, since for $\lambda = 58.4\,\mathrm{nm}$ these two states come into resonance. The period of the SSEA oscillations is $T_{\rm SSEA} = 900\,\mathrm{a.u.} = 21.2\,\mathrm{fs}$, and is equal to the theoretical Rabi value given by $T_{\rm Rabi} = \frac{2\pi}{F\langle 1s^2|z|1s2p\,{}^1P^o\rangle}$.

Figure 2 depicts $P(t)$ for $\lambda = 61.4\,\mathrm{nm}$ and $I = 10^{13}\,\mathrm{W\,cm}^{-2}$. The deduced two-photon cross section is $\sigma(2) = 9.5 \times 10^{-52}\,\mathrm{cm}^4\,\mathrm{s}$. No Rabi oscillations are present, in accordance with the fact that, for this wavelength, the ${}^1S$ ground state is not on resonance with any ${}^1P^o$ Rydberg state.

Figure 3 is our last example of the determination of $\sigma(2)$ from the fit of the computed $P(t)$. Here, $\lambda = 52.2\,\mathrm{nm}$ and $I = 10^{14}\,\mathrm{W\,cm}^{-2}$. Now, there is resonant coupling of the ${}^1S$ ground state with the $1s4p\,{}^1P^o$ Rydberg state. The period of the computed oscillations is $T_{\rm SSEA} = 908.4\,\mathrm{a.u.} = 22\,\mathrm{fs}$, which is, again, the value expected from the Rabi expression.

A. Nonlinear effects of Rydberg states

A look at Figs. 1–3 reveals an increased complexity in the structure of Fig. 3 (excitation of the $1s4p\,{}^1P^o$ state) as compared to that of Fig. 1 (excitation of the $1s2p\,{}^1P^o$ state).

The structure and methodology of the SSEA makes possible the explanation of this difference in a systematic and quantitative way. The complexity of the additional oscillations of $P(t)$ is due to the proximity of the $1s4p\,{}^1P^o$ state to other Rydberg states. These are the $1snp\,{}^1P^o$, as well as the $1sn\ell\,{}^1L$

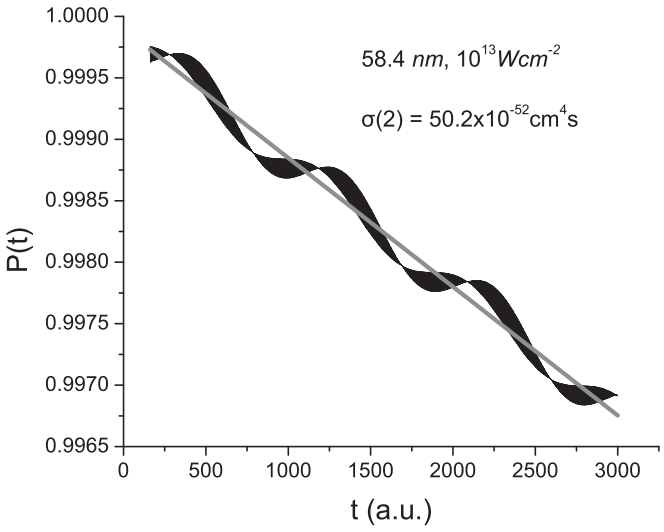

FIG. 1. The survival probability $P(t)$ for $\lambda = 58.4\,\mathrm{nm}$ and $I = 10^{13}\,\mathrm{W\,cm}^{-2}$ as a function of time in atomic units (a.u.). The thick gray line corresponds to the fitted $e^{-\Gamma t}$, with $\Gamma = 1.05 \times 10^{-6}$ a.u.. The resonant coupling of the He ground state $1s^2$ with the excited state $1s2p\,{}^1P^o$ causes a Rabi oscillation between them. The calculated period of oscillation of $P(t)$ is $T_{\rm SSEA} = 900\,\mathrm{a.u.} = 21.2\,\mathrm{fs}$, a result which is in perfect agreement with the Rabi formula.

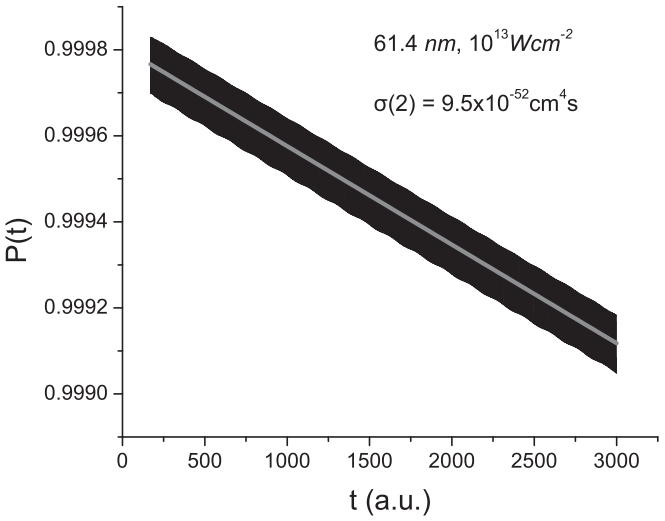

FIG. 2. As in Fig. 1, but for $\lambda = 61.4$ nm. Rabi oscillations do not exist since, for this wavelength, the ground state $1s^2$ is not resonantly connected to any excited state.

($^1L \neq {}^1P^o$), $n = 3$–7 states, all of which are coupled (including the ground state, ^1S) through the full Hamiltonian during the nonperturbative calculation.

As we explained in Sec. III, the inclusion of the state-specific Rydberg wave functions into the SSEA expansion of Eq. (2) is explicit. They are computed numerically for each value of n and ℓ. Therefore, they can be added or subtracted at will, thereby allowing the study of the influence of each one of them on the final solution.

Given the problem of interest here, we carried out a series of calculations for the case $\lambda = 52.2$ nm and $I = 1 \times 10^{14}$ W cm^{-2}, where the Rydberg states $1snl\ ^1L$, $n = \ell + 1$,..., except the $1s4p\ ^1P^o$, were removed successively. An interesting picture emerged, and this is shown in Fig. 4.

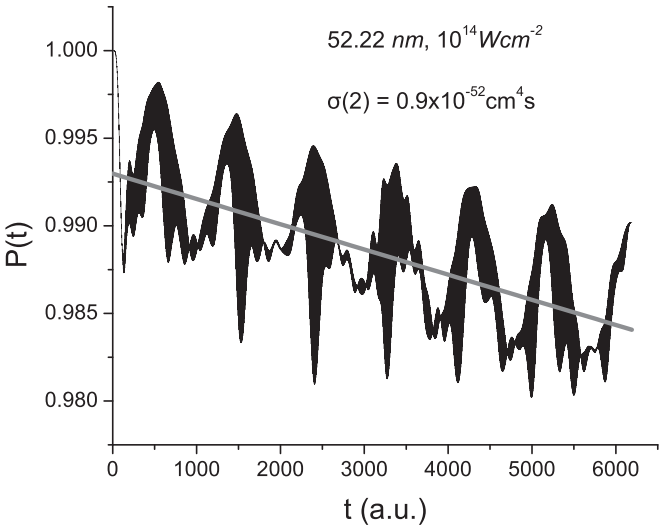

FIG. 3. As in Fig. 1, but for $\lambda = 52.2$ nm and $I = 10^{14}$ W cm^{-2}. Again, the resonant coupling of the ground state with the $1s4p\ ^1P^o$ state is manifested as oscillations of period $T_{\mathrm{SSEA}} = 908.4$ a.u. = 22 fs, which is in agreement with the Rabi formula.

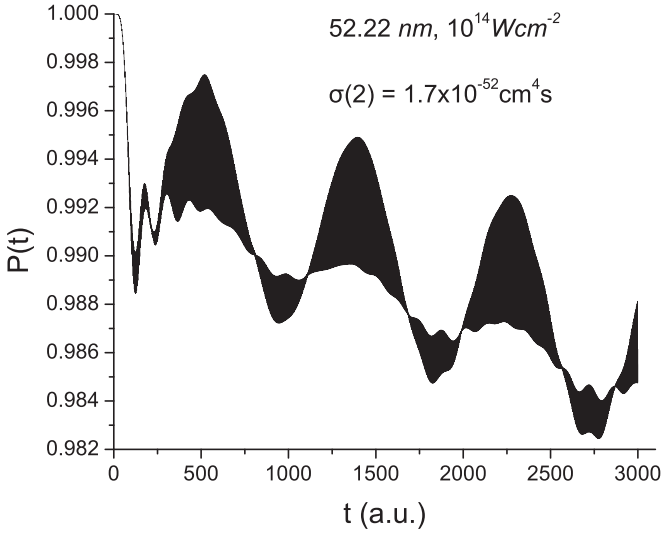

FIG. 4. As in Fig. 3, without the Rydberg states $1snl\ ^1L$, $n = \ell + 1, \ldots$, except the $1s4p\ ^1P^o$. The remaining structures, which are of small amplitude, should be attributed to the contribution of the scattering states just above threshold.

Now, the Rabi oscillations are smoother compared to those of Fig. 3. The remaining small structures should be attributed to the contribution of the scattering states just above threshold.

This computational test also demonstrates the nonlinear effect of the Rydberg series on the observable $\sigma(2)$. Specifically, when the Rydberg states $1snl\ ^1L$, $n = \ell + 1$,... are taken out (except of course the $1s4p\ ^1P^o$), the cross section from Fig. 4 is 1.7×10^{-52} cm^4 s compared to the accurate 0.9×10^{-52} cm^4 s which corresponds to Fig. 3 and is reported in Table III.

In conclusion, the calculations which led to Figs. 3 and 4 demonstrate the indirect, nonlinear effects on the time-dependent ionization probability of the Rydberg states neighboring the $1s4p\ ^1P^o$ state at $\lambda = 52.2\,nm$. Of course, it is Fig. 3, for which the calculation includes all the Rydberg states up to $n = 7$ and $\ell = 4$, that represents the accurate picture.

B. Cross sections from the SSEA, and comparison with those of the FEL experiments [1,2] and of the *R*-matrix Floquet method [4]

The SSEA results for $\sigma(2)$ are shown in Table III, where they are compared with the values from the FEL experiments [1,2] and with the results from the time-independent *R*-matrix Floquet calculations [4]. For $\lambda = 52.22$ and 51.56 nm, for which the $1s4p\ ^1P^o$ and $1s5p\ ^1P^o$ levels are on resonance, respectively, the $\sigma(2)$ of [4] were deduced from their Fig. 1, where the two-photon-ionization rates are given for $I = 1 \times 10^{13}$, 2×10^{13}, 5×10^{13}, and 1×10^{14} W cm^{-2}.

The numbers in Table III show the following. When the SSEA results are compared with the experimental values, only for two cases (1×10^{13} W cm^{-2} and $\lambda = 53.4$ nm, and 5×10^{13} W cm^{-2} and $\lambda = 58.4$ nm) is there agreement. As regards the results from the two nonperturbative calculations ([4] and the present SSEA work), there is satisfactory agreement for most cases where the intensity is 1×10^{13}, 2×10^{13}, and 5×10^{13} W cm^{-2}. For the relatively weak intensity at

TABLE III. Two-photon-ionization cross sections $\sigma(2)$ of He, for six EUV wavelengths and for intensities beyond the perturbative regime. The values from the recent FEL experiments [1,2] are compared with the results from the time-independent R-matrix Floquet calculations [4] and from the fitting of the present SSEA time-dependent probabilities to $e^{-\Gamma t}$, where Γ is the two-photon-ionization rate. Wavelengths marked with asterisks correspond to resonance frequencies with the Rydberg states, $1snp\ ^1P^o$, $n = 2,3,4,5$. In units of 10^{-52} cm^4 s.

λ (nm)	51.56*	52.22*	53.4*	56.0	58.4*	61.4
3×10^{12} W/cm^2		32.6[a]			165.8[a]	
					500[b]	
1×10^{13} W/cm^2	3.7[a]	7.4[a]	6.8[a]	3.1[a]	50.2[a]	9.5[a]
	6.1[c]	9.5[c]	6.9[c]	3.5[c]	63.0[c]	8.5[c]
			7.0[d]	0.9[d]	23.0[d]	2.6[d]
2×10^{13} W/cm^2	2.4[a]	3.8[a]	4.9[a]	3.1[a]	25.3[a]	9.2[a]
	3.7[c]	5.7[c]	5.0[c]	3.5[c]	30.0[c]	8.5[c]
			3.4[d]	0.85[d]	16.0[d]	2.4[d]
5×10^{13} W/cm^2	0.67[a]	1.8[a]	3.1[a]	2.9[a]	11.1[a]	8.8[a]
		3.3[c]	3.0[c]	3.2[c]	10.0[c]	8.0[c]
			1.4[d]	0.77[d]	10.0[d]	2.2[d]
1×10^{14} W/cm^2	0.58[a]	0.9[a]				
		1.8[c]				

[a]This work. From the solution of the METDSE using the SSEA.
[b]Fushitani *et al.* [1]. FEL experiment.
[c]van der Hart and Bingham [4]. R-matrix Floquet method.
[d]Sato *et al.* [2]. FEL experiment.

3×10^{12} W cm^{-2}, there is no R-matrix Floquet result [4] with which to compare.

When intensity is set at 1×10^{14} W cm^{-2}, we carried out two indicative calculations. For the one at 51.56 nm (on resonance with the $1s5p\ ^1P^o$ state), there is no reported result in [4], and so the SSEA number constitutes a quantitative prediction for future experiments reaching the upper Rydberg states. For the one at 52.22 nm (on resonance with the $1s4p\ ^1P^o$ state), the R-matrix Floquet value which we deduced from Fig. 1 of [4] deviates from the SSEA result by a factor of 2.

V. SYNOPSIS

Two recent experiments, both using FEL, produced *absolute* values of two-photon-ionization cross sections, $\sigma(2)$, of the helium ^1S ground state, for pulses of EUV wavelengths which are on and off resonance with the $^1P^o$ Rydberg states $1s2p$ and $1s3p$ [1,2]. The measurements of [1,2] offer the important opportunity for testing advanced theoretical methods that have been introduced in recent decades for the nonperturbative treatment and the quantitative understanding of multiphoton processes in polyelectronic atoms and molecules.

In Secs. I and II, we discussed the situation concerning the published results for the EUV $\sigma(2)$ of helium. We pointed out that the experimental results of [1] are not in satisfactory agreement with those of [2], while both sets differ quantitatively from the results of two theoretical works, one based on LOPT [3] and the other on the nonperturbative R-matrix Floquet theory [4], with which the authors of [1,2] compared their findings. The deviation from each other of most of the $\sigma(2)$ values of the four sets (two experimental and two theoretical) is so distinct that no conclusion as to their accuracy and physical relevance can be drawn without additional data (see Table I). We also presented the results from our earlier calculations using the MEMPT [5] for weak and for strong pulses in the EUV range, and compared them with the results of the FEL experiments [1,2] and of the nonperturbative method of [4] (Table II). Certain conclusions and results from [1,2,4] confirm those of the MEMPT predictions [5].

The present work is based on a time-dependent framework, and aims at determining the MPI cross sections by fitting the time-dependent ionization probabilities $P(t)$ to $e^{-\Gamma t}$. These were computed from the nonperturbative solution of the METDSE via the state-specific expansion approach (SSEA) [6,7]. The features of the state-specific N-electron basis wave functions were explained in Sec. III. For the He bound states, they were computed *numerically* at the MCHF (ground state) or HF level (Rydberg states), thereby eliminating the possibility of inaccuracies that are created when Rydberg states are represented by a single analytic basis set. The energy-normalized scattering wave functions for the He^+ $1s + \varepsilon l$ channels were computed at the frozen-core HF level for each value of the angular momentum and each value of the free-electron energy, from 0.0 to 2.0 a.u., in steps of 0.001 a.u.

Wavelengths corresponding to one-photon excitations that are off and on resonance with the $1s2p$, $1s3p$, $1s4p$, and $1s5p\ ^1P^o$ Rydberg states were considered. Using the resulting $\Psi(t)$, we computed the survival probability, $P(t)$, defined in Eq. (4). This $P(t)$ is then fitted to $e^{-\Gamma t}$, where Γ is the two-photon-ionization rate. The cross section $\sigma(2)$ is computed from Eq. (7b). For transitions on resonance, the period of oscillations of the SSEA $P(t)$ agrees quantitatively with that predicted by the Rabi formula (Figs. 1–3).

As explained and justified in Sec. III, in the present case, the SSEA formalism and implementation were generalized by making possible the calculation of bound-bound, bound-free, and free-free coupling matrix elements of the full electric operator of the *multipolar* Hamiltonian, Eq. (5). The calculations were carried out subject to the electric-dipole selection rules, which generate the overwhelmingly dominant parts of the free-free matrix elements [12,13].

The numerical values for the SSEA $\sigma(2)$ and their comparison with those from the experiments [1,2] and from the theory of [4] are presented in Table III. The values for the weak field 3×10^{12} W/cm^2 at $\lambda = 52.22$ nm (on resonance with the $1s4p\ ^1P^o$ state), and for the strong fields 5×10^{13} W/cm^2 and 1×10^{14} W/cm^2 at $\lambda = 51.56$ nm (on resonance with the $1s5p\ ^1P^o$ state), are predictions of this work. They can serve as reference numbers in future FEL experiments.

[1] M. Fushitani, Y. Hikosaka, A. Matsuda, T. Endo, E. Shigemasa, M. Nagasono, T. Sato, T. Togashi, M. Yabashi, T. Ishikawa, and A. Hishikawa, Nonresonant EUV-UV two-color two-photon ionization of He studied by single-shot photoelectron spectroscopy, Phys. Rev. A **88**, 063422 (2013).

[2] T. Sato, A. Iwasaki, K. Ishibashi, T. Okino, K. Yamanouchi, J. Adachi, A. Yagishita, H. Yazawa, F. Kannari, M. Aoyma, K. Yamakawa, K. Midorikawa, H. Nakano, M. Yabashi, M. Nagasono, A. Higashiya, and T. Ishikawa, Determination of the absolute two-photon ionization cross section of He by an XUV free electron laser, J. Phys. B: At., Mol. Opt. Phys. **44**, 161001 (2011).

[3] L. A. A. Nikolopoulos and P. Lambropoulos, Multichannel theory of two-photon single and double ionization of helium, J. Phys. B **34**, 545 (2001).

[4] H. W. van der Hart and P. Bingham, Two- and three-photon ionization of He between 10^{13} and 10^{14} W cm^{-2}, J. Phys. B **38**, 207 (2005).

[5] T. Mercouris, S. I. Themelis, and C. A. Nicolaides, Non-perturbative theory and computation of the nonlinear response of He to dc and ac fields, Phys. Rev. A **61**, 013407 (1999).

[6] T. Mercouris, Y. Komninos, and C. A. Nicolaides, The state-specific expansion approach and its application to the quantitative analysis of time-dependent dynamics in atoms and small molecules, Adv. Quantum Chem. **60**, 333 (2010).

[7] C. A. Nicolaides, Quantum chemistry on the time axis: Electron correlations and rearrangements on femtosecond and attosecond scales, Mol. Phys. **114**, 453 (2016).

[8] C. A. Nicolaides, State- and property-specific quantum chemistry, Adv. Quantum Chem. **62**, 35 (2011).

[9] C. A. Nicolaides, S. Dionissopoulou, and T. Mercouris, The significance of electron correlation and of state symmetries in the interaction of strong laser pulses of 5 eV with He, J. Phys. B **31**, L1 (1998).

[10] R. Loudon, *The Quantum Theory of Light*, 2nd ed. (Clarendon, Oxford, 1983).

[11] D. P. Craig and T.Thirunamachandran, *Molecular Quantum Electrodynamics* (Dover, Mineola, NY, 1998).

[12] Y. Komninos, T. Mercouris, and C. A. Nicolaides, On- and off-resonance radiation-atom-coupling matrix elements involving extended atomic wave functions, Phys. Rev. A **89**, 013420 (2014).

[13] Y. Komninos, T. Mercouris, and C. A. Nicolaides, Theory and computation of electromagnetic transition matrix elements in the continuous spectrum of atoms, Eur. Phys. J. D (to be published).

[14] W. Pauli, *General Principles of Quantum Mechanics* (Springer-Verlag, Berlin, 1980).

[15] D. H. Kobe and K. H. Yang, Gauge transformation of the time-evolution operator, Phys. Rev. A **32**, 952 (1985).

[16] W. E. Lamb, R. R. Schlicher, and M. O. Scully, Matter-field interaction in atomic physics and quantum optics, Phys. Rev. A **36**, 2763 (1987).